NPS - 59MX70061A

United States
Naval Postgraduate School

AN ANALYTICAL AND EXPERIMENTAL INVESTIGATION OF ROTATING, NON-CAPILLARY HEAT PIPES

ANNUAL REPORT

by

P. J. MARTO
T. J. DALEY
L. J. BALLBACK

30 JUNE 1970

NAVAL POSTGRADUATE SCHOOL
Monterey, California

Rear Admiral R. W. McNitt, USN
Superintendent

R. F. Rinehart
Academic Dean

ABSTRACT

An analytical review of the operation of rotating, non-capillary heat pipes is presented, including a discussion of film condensation on the inside of a rotating, truncated cone. Predicted results so far obtained indicate that the heat transfer capability of rotating, non-capillary heat pipes depends upon condenser performance and is substantially higher than the capability of conventional, wick-limited heat pipes.

The design and manufacture of an experimental rotating heat pipe apparatus is also described.

This task was supported by:

NATIONAL AERONAUTICS AND SPACE ADMINISTRATION
Defense Purchase Request W - 13,007

Prepared by: P. J. Marto

P. J. Marto
Associate Professor of
Mechanical Engineering
L. J. Ballback, LT., USN
T. J. Daley, LTJG., USN

Approved by: T. Sarpkaya

T. Sarpkaya
Chairman, Department of
Mechanical Engineering

Released by: C. E. Menneken

C. E. Menneken
Dean of
Research Administration

NPS - 59MX70061A
30 June 1970

TABLE OF CONTENTS

		Page
1.	INTRODUCTION	1
	1.1 Conventional Heat Pipe	1
	1.2 The Rotating, Non-Capillary Heat Pipe	2
	1.3 Objective	3
2.	STATUS OF ANALYTICAL PROGRAM	4
	2.1 Limits of Operation	4
	2.2 Film Condensation Theory	5
3.	STATUS OF EXPERIMENTAL PROGRAM	14
	3.1 Description of Equipment	14
4.	SUMMARY OF WORK PERFORMED	21
	4.1 Analytical Program	21
	4.2 Experimental Program	22
5.	PROPOSED ACTIVITIES	23
	5.1 Analytical Program	23
	5.2 Experimental Program	23
BIBLIOGRAPHY		24
INITIAL DISTRIBUTION LIST		40
FORM DD 1473		45

1. INTRODUCTION

1.1 CONVENTIONAL HEAT PIPE

A heat pipe is a self-contained device which can transport large quantities of heat at nearly isothermal conditions. Conventionally, it consists of three main parts: a container, a working fluid, and a capillary wicking structure which is saturated with the working fluid.

When heat is added to one end of the container, some of the working fluid evaporates. The resulting vapor flows to the opposite end of the container, transporting heat as latent heat of vaporization. Here the vapor condenses on the cooler surface and releases the heat to be removed from the structure. The condensate is pumped back to the evaporator section by capillary action within the wicking structure, thus completing the cycle. The heat pipe is unique in that it operates with no moving parts, maintains nearly isothermal conditions, and removes the dependency on gravity through the use of capillary pumping.

Limits on the heat transfer capabilities of conventional heat pipes are imposed by a number of fluid-dynamic mechanisms, including a wick resistance limit, a sonic vapor velocity limit, a vapor velocity entrainment limit, and also a wick boiling limit [1,2,3,].* In each case, the heat transfer

---

*Numbers in brackets indicate references listed in the Bibliography.

limit is defined to occur when the wick begins to dry out in the evaporator, causing excessive operating temperatures there. These limits have been considered in a number of studies [4,5,6] with the conclusion that, in general, a conventional heat pipe using an ordinary working fluid is limited by the rate that the condensate can be returned to the evaporator due to wick resistance. Under certain circumstances, nucleate boiling in the wick structure may also limit operation.

1.2 THE ROTATING, NON-CAPILLARY HEAT PIPE

The wick-resistance and boiling limitations of conventional heat pipes can be overcome by removing the wick and by utilizing centrifugal acceleration to return the condensate to the evaporator [7].

The rotating, non-capillary heat pipe is shown schematically in FIGURE 1. It consists of a sealed, hollow shaft, having a slight internal taper from one end to the other, and containing a fixed amount of working fluid. When the shaft is rotated at high speed about its longitudinal axis, the working fluid collects as an annulus at the large end. Heat added to this end of the shaft (evaporator) evaporates the working fluid, generating vapor which then flows axially toward the other end. Heat removed from this end of the shaft (condenser) condenses the vapor. The centrifugal forces accelerate the liquid condensate back to the evaporator to complete the cycle.

By removing the wick structure, its limitations on heat transfer capability are also removed. The rotating, non-capillary heat pipe can therefore operate at much higher heat fluxes than conventional heat pipes and has many potential applications [7].

1.3 OBJECTIVE

The overall objective of this research program is to analytically study the operation of rotating, non-capillary heat pipes and to experimentally test the performance of these devices.

This annual report describes the work performed through 30 June 1970 under NASA Defense Purchase Request W-13,007 for the Lewis Research Center, Cleveland, Ohio.

2. STATUS OF ANALYTICAL PROGRAM

2.1 LIMITS OF OPERATION

In a preliminary analysis of the operation of a rotating, non-capillary heat pipe, Ballback [8] studied the limitations of various fluid-dynamic mechanisms which may be imposed on the rotating pipe. Using existing theoretical equations and experimental correlations, he estimated the limitations imposed by (a) the critical nucleate boiling heat flux ("burnout"), (b) the entrainment of the condensate ("flooding"), and (c) the sonic vapor velocity. In addition, he estimated a condensing limitation by performing a simplified Nusselt film condensation analysis. He modeled the condenser section of the heat pipe as a rotating, truncated cone which had no external thermal resistance. His approximate analytical expression is applicable to ordinary fluids and can be used to study the influence of rotational speed, condenser internal geometry and fluid properties upon rotating heat pipe performance.

Ballback compared his four proposed limitations for a 14.0-inch long rotating heat pipe with a minimum inside diameter of 2.0-inches and a half-cone angle of 1 degree. His estimated results are re-plotted in FIGURE 2 for a 1/8-inch thick stainless steel heat pipe operating with water at 2700 RPM. From these results, two conclusions were drawn. First of all, the rotating, non-capillary heat pipe will transfer significantly more heat than

a conventional heat pipe. Secondly, even with the associated uncertainties in each of the four above-mentioned limitations, the rotating, non-capillary heat pipe will be condensation limited. Thus, its performance will be controlled by the amount of heat that can be removed from the condenser section.

It was therefore concluded that it would be important to more thoroughly study and understand the condensation mechanism within rotating, non-capillary heat pipes in an effort (a) to reliably predict their behavior, and (b) to improve upon their performance.

2.2 FILM CONDENSATION THEORY

In analyzing the condensation mechanism within the rotating heat pipe, it was assumed that film condensation and not dropwise condensation occurs. Thus, the working fluid was assumed to completely wet the inside surface of the condenser and spread out into a thin condensate film.

The film condensation mechanism within the rotating heat pipe is complicated by the dynamical flow interactions between the liquid and the vapor during rotation. Such effects as swirl of the condensate, interfacial shear between the condensate and the vapor, axial pressure drop of the vapor, and formation of waves or ripples in the condensate may be important. It was reasoned that inclusion of these mechanisms into an initial analytical program would serve to complicate the analysis without improving upon the understanding of rotating heat pipe operation. On the other hand,

a fundamental laminar film condensation analysis (similar to Nusselt's classical analysis [9])would establish an analytical reference solution which would be applicable to ordinary fluids. This solution could be verified experimentally and could be modified during the latter portion of this research project to include the above-mentioned mechanisms. In so doing, the relative importance of each of these mechanisms could be evaluated individually, leading perhaps to important design changes and to improved heat pipe performance.

Prior to this investigation, there was no complete solution for laminar film condensation on the inside of a rotating, truncated cone. In searching the literature, however, it was discovered that in 1961, Sparrow and Hartnett [10] carried out a solution for laminar film condensation on the outside of a rotating cone. They used a boundary layer approach and pointed out that their similarity solution applies only to cones that are not too slender. They obtained a condensate film thickness which remains uniform along the condenser surface, but which depends on liquid Prandtl Number, Pr, and on the parameter $C_p(T_s-T_w)/h_{fg}$. For ordinary fluids with Prandtl Numbers near unity, and for $C_p(T_s-T_w)/h_{fg}<0.1$, they found that the film thickness could be predicted by:

$$\delta = 1.107\left[\frac{c_p(T_s-T_w)}{Pr\ h_{fg}}\right]\sqrt{\frac{\nu}{\omega \sin\phi}} \qquad (1)$$

In the above equation,

C_p = specific heat of the condensate

T_s = saturation temperature of the vapor

T_w = condenser wall surface temperature

h_{fg} = latent heat of vaporization

ν = kinematic viscosity of the condensate

ω = angular velocity of the condenser, and

ϕ = one half the internal cone angle (half-cone angle).

Their similarity solution was applied during this project to the inside of a rotating, truncated cone with a geometry defined in FIGURE 3. This analysis led to the same expression for the film thickness as predicted by eq'n. (1). When the thermal resistance across the condensate film was included with the condenser wall resistance and the outside cooling thermal resistance, a simple expression for the overall heat removal rate from the condenser (which in steady state must be the heat transport rate of the heat pipe) was derived:[1]

$$Q_t = \frac{2\pi L_c (T_s - T_\infty)(R_o + \frac{L_c}{2}\sin\phi)}{\frac{\delta}{k_f} + \frac{t}{k_w} + \frac{1}{h}} \qquad (2)$$

[1] Equation (2) is valid for thin condensate films and condenser walls.

where

T_∞ = outside ambient fluid temperature

h = outside heat transfer coefficient (which depends on the exterior cooling mechanism)

t = condenser wall thickness

k_w = thermal conductivity of the condenser wall

k_f = thermal conductivity of the condensate

and where R_o, L_c and ϕ are defined in FIGURE 3. Note that in eq'n (1) the inside wall surface temperature T_w is not generally known, but depends on Q_t and δ from the heat transfer rate across the condensate film:

$$Q_t = \frac{2\pi L_c k_f (R_o + \frac{L_c}{2} \sin\phi)(T_s - T_w)}{\delta} \qquad (3)$$

Equations (1), (2) and (3) were solved simultaneously for water condensing on the inside of a stainless steel condenser surface for which

R_o = 0.730 inches

L_c = 9.0 inches

t = 0.0625 inches, and

ϕ = 1, 2 and 3 degrees .

The outside heat transfer coefficient was assumed to be $h = 500$ BTU/hr ft^2 °F and $h = \infty$. The results at atmospheric pressure for various rotational speeds are plotted as dashed curves in FIGURES 4, 5 and 6. Note that the heat removal rate, Q_t increases

with rotational speed and half-cone angle, ϕ. Note also that Q_t depends strongly on the selection of the outside heat transfer coefficient, h.

This similarity solution, as pointed out earlier, pertains only to large cone angles and must therefore be approximate for small half-cone angles ϕ = 1, 2 and 3 degrees. In addition, it leads to a condensate velocity distribution given by

$$u(x,y) = \frac{\rho_f \omega^2}{\mu_f}\left(\delta y - \frac{y^2}{2}\right)(R_o + x\sin\phi)\sin\phi \qquad (4)$$

where

ρ_f = density of the condensate, and

μ_f = dynamic viscosity of the condensate.

This velocity does not satisfy the boundary condition that along the condenser end wall at x = 0(y>0), the velocity must be zero.[2]

In an effort to overcome these restrictions, Ballback performed a Nusselt-type analysis for film condensation on the inside of a rotating, truncated cone [8]. Using the coordinate system shown in FIGURE 3 and following the classical assumptions used by Nusselt, he found that the condensate velocity could be expressed by

$$u(x,y) = \frac{\rho_f \omega^2}{\mu_f}\left(\delta y - \frac{y^2}{2}\right)(R_o + x\sin\phi - \delta\cos\phi)\left(\sin\phi - \cos\phi\frac{d\delta}{dx}\right) \qquad (5)$$

---

[2] Strictly speaking, because of the heat pipe geometry and coordinate system chosen in FIGURE 3, the condensate velocity is very small but not exactly zero at x = 0, y>0.

Equation (5) reduces to eq'n (4) if the condensate film is very thin (i.e., $\delta \cos \phi << R_o + x \sin \phi$) and if the slope of the condensate film, $\frac{d\delta}{dx}$ is much less than $\tan \phi$. The first of these assumptions will be true under most circumstances. However, the second assumption will only be satisfied for cones which are not too slender.

Ballback made both of these assumptions in his analysis in order to analytically solve for the film thickness. He used the boundary condition, however, that δ must be zero at $x = 0$ to satisfy the initial condition on the velocity, and arrived at the following solution for the film thickness

$$\delta(x) = 1.107\left[\frac{c_p(T_s - T_w)}{P_r\, h_{fg}}\right]\sqrt{\frac{\nu}{\omega \sin\phi}}\left\{1 - \left(\frac{R_o}{R_o + x\sin\phi}\right)^{8/3}\right\}^{1/4} \quad (6)$$

This equation differs from eq'n (1) because of its explicit dependence on x, and predicts an average film thickness which is less than that predicted by Sparrow and Hartnett [10].

Daley [11] modified Ballback's work to include the thermal resistances in the condenser wall and in the outside surface cooling mechanism. Daley numerically integrated for the heat removal rate Q_t using the same boundary condition as Ballback, that at $x = 0$, $\delta = 0$. His results are plotted as the solid curves in FIGURES 4, 5 and 6 for the same heat pipe geometry and operating conditions

as the Sparrow and Hartnett results. Notice that Daley's results are substantially higher than those predicted by the Sparrow and Hartnett similarity solution. This is due presumably to the thinner film thickness which results in Daley's analysis from the boundary condition that at $x = 0$, $\delta = 0$. Since both results, however, are limited to large half-cone angles, the curves shown in FIGURES 4, 5 and 6 remain approximate for cones represented by $\phi = 1$, 2 and 3 degrees.

The restriction of large half-cone angles was later removed by Daley [11]. Using the condensate velocity profile given by eq'n (5) and keeping in all the terms, he arrived at a second-order, non-linear differential equation for the film thickness:

$$\frac{2\pi \rho_f^2 \omega^2 h_{fg}}{\mu_f}\left\{\left(\sin\phi - \cos\phi\frac{d\delta}{dx}\right)^2\left(\frac{\delta^3}{3}(R_o + x\sin\phi) - \frac{5}{24}\delta^4\cos\phi\right)\right.$$

$$+ \left(R_o + x\sin\phi - \delta\cos\phi\right)\left(\frac{\delta^3}{3}(R_o + x\sin\phi) - \frac{5}{24}\delta^4\cos\phi\right)\left(-\frac{d^2\delta}{dx^2}\cos\phi\right)$$

(7)

$$\left.+\left(R_o + x\sin\phi - \delta\cos\phi\right)\left(\sin\phi - \cos\phi\frac{d\delta}{dx}\right)\left(\delta^2\frac{d\delta}{dx}(R_o + x\sin\phi) + \frac{\delta^3}{3}\sin\phi - \frac{5}{6}\delta^3\frac{d\delta}{dx}\cos\phi\right)\right\}$$

$$= \frac{2\pi (R_o + x\sin\phi)(T_s - T_\infty)}{\frac{\delta}{K_f} + \frac{t}{K_w} + \frac{1}{h}}$$

where the right-hand side of this expression is just the rate of change of the heat transport rate, $\frac{dQ_t}{dx}$. Equation (7) is valid for all half-cone angles, and reduces upon simplification to existing theoretical expressions for both a rotating disc [12] at $\phi = 90°$ and for a rotating cylinder [13] at $\phi = 0°$.

Daley numerically integrated this expression using a Runge-Kutta-Gill numerical integration scheme with an IBM 360 Mod 67 digital computer. To start the integration, the following initial values were selected at x = 0:

$$\delta = \delta_i \qquad (8a) \quad \text{, and}$$

$$\frac{d\delta}{dx} = \tan \phi \qquad (8b)$$

From eq'n (5), $\frac{d\delta}{dx}$ must be equal to tan ϕ at x = 0(y>0) in order to satisfy the initial condition for the condensate velocity. However, the initial value of the film thickness δ_i is unknown and is believed to depend on the minimum film thickness δ_{min} which occurs at or very near the exit of the condenser. Thus, as stated by Leppert and Nimmo [13] for condensation on finite surfaces normal to inertial forces, the starting film thickness at x = 0 is determined by the minimum film thickness δ_{min}. They postulate that the minimum thickness depends on the particular overfall condition which occurs at the surface's edge. This dependence is shown schematically in FIGURE 7. Daley used a free overfall condition (as derived in open channel flow) to approximate the flow over the

corner at the condenser exit. He arrived at a minimum condensate thickness given by:

$$\delta_{min} = \left[\frac{0.7\ \dot{m}_f^2}{(2\pi \rho_f \omega)^2 (R_o + L_c \sin\phi)^3} \right]^{1/3} \qquad (9)$$

where $\dot{m}_f$ is the mass flow rate of the condensate at the exit of the condenser. He therefore assumed an initial value for δ_i and integrated his equations out to $x = L_c$. Using his integrated film thickness, he solved for $\dot{m}_f$ at $x = L_c$ and used this result in eq'n (9) to get δ_{min}. He then compared δ_{min} to his film thickness at $x = L_c$. If the two thicknesses agreed to within .0004 inches, a solution was obtained. If the two thicknesses did not agree, a new starting value of δ_i was assumed and the integration scheme repeated.

Daley applied this technique to a rotating cylinder with a half-cone angle $\phi = 0°$. His results for $R_o = 0.730$ inches, $L_c = 9.0$ inches and $t = 0.0625$ inches are plotted in FIGURE 8 for two values of the outside heat transfer coefficient, $h = 500$ BTU/hr ft^2 °F and $h = \infty$. Note that this chosen rotating heat pipe is attractive even without an internal taper. For example, at an RPM of 2400, with an outside heat transfer coefficient of 500 BTU/hr ft^2 °F, this rotating heat pipe can still transfer about 3 KW of power. Results for half-cone angles greater than zero have not yet been obtained.

3. STATUS OF EXPERIMENTAL PROGRAM

In order to test rotating, non-capillary heat pipe performance, an experimental apparatus was designed, manufactured, and partially assembled.

In designing the equipment, the evaporator section was modeled after the rotating boiler apparatus which has been used at the Lewis Research Center for the study of boiling heat transfer coefficients at high gravity levels [14,15]. The condenser geometry was chosen to conform to the geometry used in the Analytical Program (See FIG. 3). In addition to safety and flexibility, a strong influence in the overall design was the desire to visually observe the mechanisms that will occur within the heat pipe during operation.

3.1 DESCRIPTION OF EQUIPMENT

The main components of the rotating, non-capillary heat pipe are grouped into the evaporator, condenser, auxiliary equipment, and instrumentation. FIGURE 9 is a schematic diagram of the test apparatus. A cross-sectional drawing of the assembled heat pipe is pictured in FIGURE 10, and FIGURE 11 is a photograph of the machined pieces of the rotating heat pipe prior to assembly.

Evaporator

The evaporator is a 3.125-inch inside diameter stainless steel cylinder, 5.90-inches long. One end is flanged to an outside diameter of 5.906-inches to accommodate the condenser and to support

a large, single row precision ball bearing. The other end is flanged to an outside diameter of 4.50-inches to accommodate two pyrex glass end windows. The inner window presses against a teflon-coated metallic o-ring and is separated from the outer window by a compressed fiber gasket. Both windows are held in place by a stainless steel end cap. (See FIG. 10.)

The evaporator is helically wound with an 11-gage Chromel-A heater wire in a 3/16-inch outside diameter Inconel sheath. The heater coils are silver soldered in place. They are coated with a thin layer of Sauereisen cement and are packed with asbestos insulation to reduce radial heat losses. In addition, a 1/16-inch wide radial groove is machined into the evaporator wall on either end of the heater element to reduce axial heat losses. Electrical power to the heater is passed by a graphite brush assembly through bronze collector rings. The power supply is a DC motor-generator capable of delivering 150 amperes at 250 volts.

A photograph of the machined evaporator section is shown in FIGURE 12.

Condenser

The condenser is a 10.0-inch long stainless steel, truncated cone with a 3 degree half-cone angle and with a 1/16-inch wall thickness. The large end of the condenser is flanged to bolt to the evaporator and has an inside diameter of 2.50-inches. The small end is machined into a cylinder 1.46-inches inside diameter, by 1.50-inches

long. It is flanged to accommodate a cylindrical end plug. Each flanged joint is sealed with a teflon-coated, metallic o-ring.

The stainless steel condenser end plug is hollowed out to allow the pressure transducer arm to be passed through its inside face, and to allow the drive shaft to be threaded and keyed in place. The outer end of the plug is machined down to four flat sides, each 7/8-inch wide and 7/8-inch long to accommodate phenolic thermocouple junction boards.

A photograph showing the condenser and end plug prior to assembly may be seen in FIGURE 13.

Auxiliary Equipment

The auxiliary equipment are grouped into the drive assembly, test stand, spray cooling assembly and safety shields.

Drive Assembly. The drive assembly consists of the drive shaft, support bearing, pulley and variable drive motor. The drive shaft is a 3/4-inch diameter stainless steel cylinder which is hollowed out to allow the instrumentation leads to be connected to the slip-ring unit. The outside diameter of the shaft is stepped in several places to thread into the condenser end plug, to accommodate a 2.65-inch diameter drive pulley, and to support a double row, angular contact bearing. Each end of the shaft is internally threaded. The pressure transducer arm is screwed into one end and the slip-ring coupling into the other. The shaft is screwed securely into the condenser end plug and is keyed in place. Torque is applied to

the shaft by a V-belt using a 2 HP, 3 phase variable speed motor. The motor is capable of speeds from 450 to 4500 RPM and is equipped with a magnetic disc brake and an electric remote control unit.

Test Stand. The test stand was designed so that the rotating heat pipe could be rigidly supported and tested with its longitudinal axis oriented from 0 to 90 degrees from the horizontal. Both the heat pipe assembly and the variable drive motor are bolted into steel support plates which are welded to a 4-inch diameter iron pipe. This support pipe is held in place by three 2-inch thick steel clamps which are supported 2 feet off the ground by a 1/4-inch steel welded structure. The support pipe (with the heat pipe assembly and drive motor rigidly attached as a unit) can be turned to any orientation and clamped securely in place prior to heat pipe operation. FIGURE 14 shows a photograph of the heat pipe assembly and variable drive motor mounted on the test stand.

Spray Cooling Assembly. The rotating heat pipe condenser is cooled by spraying a fine mist of tap water onto its outside surface during rotation. The spray cooling assembly is two stationary, 13-inch diameter, stainless steel half-cylinders with welded ends. These two half-cylinders completely enclose the condenser section of the heat pipe. The bottom half-cylinder is bolted to the steel support plate on which the heat pipe is mounted. The top half-cylinder is bolted to the bottom half after the heat pipe is in place and ready for operation. When mounted, each end of the half-cylinders fits

within 1/8-inch deep grooves machined into the condenser end flanges, and is sealed with a felt gasket.

Each half-cylinder contains four spray nozzles which are mounted at the same axial position but at different circumferential positions. Using various nozzles, droplet sizes ranging from 300 to 600 microns can be obtained. The cooling water is fed from copper lines to a stainless steel mixing tube soldered onto the top half-cylinder. The coolant flows from the mixing tube through plastic tubing to each of the spray nozzles. It drains through the bottom half-cylinder and is collected by a second mixing tube before being dumped to the building drain lines.

Safety Shields. To ensure safe operation, the entire heat pipe is surrounded by 1/8-inch thick stainless steel shielding which easily bolts to the steel support plate.

Instrumentation

Eight copper-constantan thermocouples were selected to be used on the rotating heat pipe. These thermocouples are 1/16-inch in diameter, Inconel sheathed, and magnesium oxide insulated, and were calibrated at 212°F, 500°F and 700°F by the Thermoelectric Company. Four of the thermocouples will be placed within 1/16-inch diameter drilled wells at different radial positions within the evaporator wall to monitor the radial heat transfer into the evaporator. One thermocouple will be suspended in the liquid annulus of the evaporator to measure the bulk liquid temperature.

Another thermocouple will be suspended in the vapor space at the evaporator exit to measure the saturation temperature of the vapor. Two additional thermocouples will be soldered into the wall of the condenser at different axial positions to monitor the heat transfer through the condenser. The leads from these thermocouples will be brought along the sides of the condenser and through the small rear condenser flange to the phenolic junction boards on the condenser end plug. From the junction boards, the leads will go inside the shaft to the slip-ring unit. The temperature of the spray coolant will be measured in the inlet and exit condenser mixing tubes using two quartz thermometers.

The saturation pressure of the vapor will be measured by a 1/4-inch diameter semi-conductor pressure transducer mounted in the vapor space. The transducer is temperature compensated and will be threaded on a 1/4-inch diameter transducer arm that extends from the drive shaft through the end plug and into the vapor space. The transducer leads will pass along the transducer arm, out through the shaft to the junction boards, and back into the shaft to the slip-rings. The pressure of the spray coolant will be indicated by a pressure tap on the coolant feed line. The spray coolant flow rate will be measured with a rotameter prior to spraying.

The rotational speed of the heat pipe will be found using both a Hewlett-Packard optical tachometer with a frequency counter and an electronic strobe light.

The electrical power into the evaporator will be measured using a calibrated voltmeter, ammeter combination. The power level will be controlled by a field rheostat placed in parallel with the DC motor-generator.

All the rotating instrumentation leads will be attached to a 22 terminal mercury slip-ring unit which is rated at less than 10 microvolts noise at speeds to 4000 RPM. The slip-ring output will be fed to a Hewlett-Packard 2010 C Data Acquisition System which has an accuracy of ± 0.5 microvolts.

4. SUMMARY OF WORK PERFORMED

4.1 ANALYTICAL PROGRAM

A preliminary analysis was performed on the operation of the rotating, non-capillary heat pipe. Nusselt's film condensation theory was extended to include centrifugal accelerations on the inside of a rotating, truncated cone. An approximate condensation limit was derived for ordinary fluids and compared to the boiling, entrainment and sonic limits for water using a given heat pipe geometry. The results indicate the rotating heat pipe to be condensation limited.

Approximate film condensation heat transfer results from the Nusselt-type analysis were substantially higher than those obtained from the modified similarity solution of Sparrow and Hartnett [10] for half-cone angles ϕ = 1, 2 and 3 degrees. An improved numerical solution was established which is valid for all half-cone angles, and which includes the thermal resistances in the condenser wall and in the outside cooling mechanism. This solution depends upon knowledge of the condensate film thickness at the exit of the condenser. Results have been obtained for a rotating cylinder with no internal taper (i.e., $\phi = 0°$) and show a strong dependence of the heat removal rate on the outside heat transfer coefficient. Results have not yet been obtained for half-cone angles greater than zero.

4.2 EXPERIMENTAL PROGRAM

The design and manufacture of a safe, flexible heat pipe apparatus was completed. A stainless steel, rotating, non-capillary heat pipe was designed so that the condenser geometry, the test fluid or the condenser outside cooling method can be varied. It was also designed for operation in any orientation with respect to gravity.

The evaporator is a 5.90-inch long cylinder with a 3.125-inch inside diameter. The condenser is a 10.0-inch long truncated cone with an internal half-cone angle of 3 degrees. The heat pipe is capable of rotational speeds to 4000 RPM, and contains a 30 KW DC-heater and a pyrex glass end window.

It is instrumented with eight copper-constantan thermocouples and a semi-conductor pressure transducer which will be monitored with a 22-terminal mercury slip-ring unit and a data acquisition system.

5. PROPOSED ACTIVITIES

5.1 ANALYTICAL PROGRAM

1. The improved Nusselt film condensation analysis, using a free overfall boundary condition at the condenser exit, will be extended to other condenser cone geometries.
2. The importance of the condensate film thickness at the condenser exit, and the importance of the free overfall boundary condition upon the condenser heat transfer rate, will be further studied.
3. An attempt will be made to investigate the effects of liquid-vapor interfacial shear, and condensate surface waves or ripples upon rotating heat pipe operation.

5.2 EXPERIMENTAL PROGRAM

1. The assembly of all the heat pipe components will be completed.
2. The heat pipe will be tested in a horizontal orientation at different rotational speeds using water, alcohol and freon.
3. Similar tests will be made with a different condenser half-cone angle.
4. It may become necessary to repeat several water heat pipe tests using different condenser exit designs to experimentally investigate what influence the condensate overfall condition may have on heat pipe operation.

BIBLIOGRAPHY

1. Cotter, T. P., "Theory of Heat Pipes", Los Alamos Scientific Laboratory Report, LA-3246-MS, February, 1965.

2. Marcus, B. D., "On the Operation of Heat Pipes", TRW Space Technology Laboratories Report, May, 1965.

3. Los Alamos Scientific Laboratory Quarterly Status Report, LA-4109-MS, February, 1969.

4. Carnesale, A., Cosgrove, J. H. and Ferrell, J. K., "Operating Limits of the Heat Pipe", AEC/SANDIA Heat Pipe Conference, Vol. 1, October, 1966.

5. Busse, C. A., "Heat Pipe Thermionic Converter Research in Europe", Paper presented at the 4th Intersociety Energy Conversion Engineering Conference, Washington, D.C., September, 1969.

6. Marto, P. J. and Mosteller, W. L., "Effect of Nucleate Boiling on the Operation of Low Temperature Heat Pipes", ASME Paper No. 69-HT-24, presented at the ASME-AIChE 11th National Heat Transfer Conference, Minneapolis, Minnesota, August, 1969.

7. Gray, V. H., "The Rotating Heat Pipe - A Wickless Hollow Shaft for Transferring High Heat Fluxes", ASME Paper No. 69-HT-19, presented at the ASME-AIChE 11th National Heat Transfer Conference, Minneapolis, Minnesota, August, 1969.

8. Ballback, L. J., "The Operation of a Rotating, Wickless Heat Pipe", M.S. Thesis, Naval Postgraduate School, Monterey, California, December, 1969.

9. Nusselt, W., "Die Oberflächenkondensation des Wasserdampfes", Z. Ver. Deutsch. Ing., 60, pp. 541-569, 1916.

10. Sparrow, E. M. and Hartnett, J. P, "Condensation on a Rotating Cone", Journal of Heat Transfer, 83, pp 101-102, February, 1961.

11. Daley, T. J., "The Experimental Design and Operation of a Rotating, Wickless Heat Pipe", M. S. Thesis, Naval Postgraduate School, Monterey, California, June, 1970.

12. Sparrow, E. M. and Gregg, J. L., "A Theory of Rotating Condensation", Journal of Heat Transfer, 81, pp. 113-120, May, 1959.

13. Leppert, G. and Nimmo, B. G., "Laminar Film Condensation on Surfaces Normal to Body or Inertial Forces", Journal of Heat Transfer, 90, pp. 178-179, February, 1968.

14. Gray, V. H., Marto, P. J. and Joslyn, A. W., "Boiling Heat Transfer Coefficients, Interface Behavior, and Vapor Quality in Rotating Boiler Operating to 475 G's", NASA- TN D-4136, March, 1968.

15. Marto, P. J. and Gray, V. H., "Effects of Acceleration on Nucleate Boiling of Water in a Rotating Boiler", NASA Technical Note (To be published).

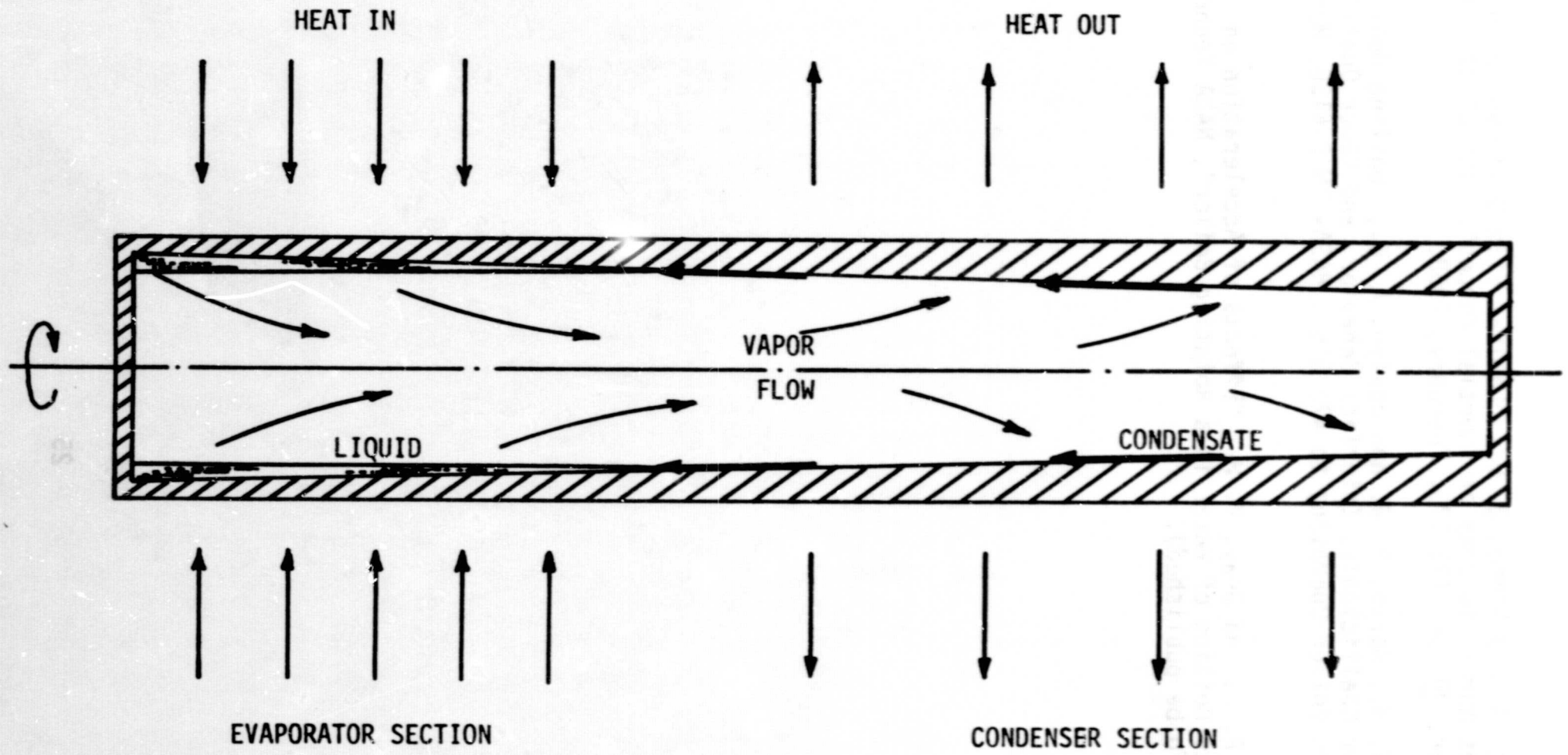

FIGURE 1 SCHEMATIC DRAWING OF ROTATING, NON-CAPILLARY HEAT PIPE

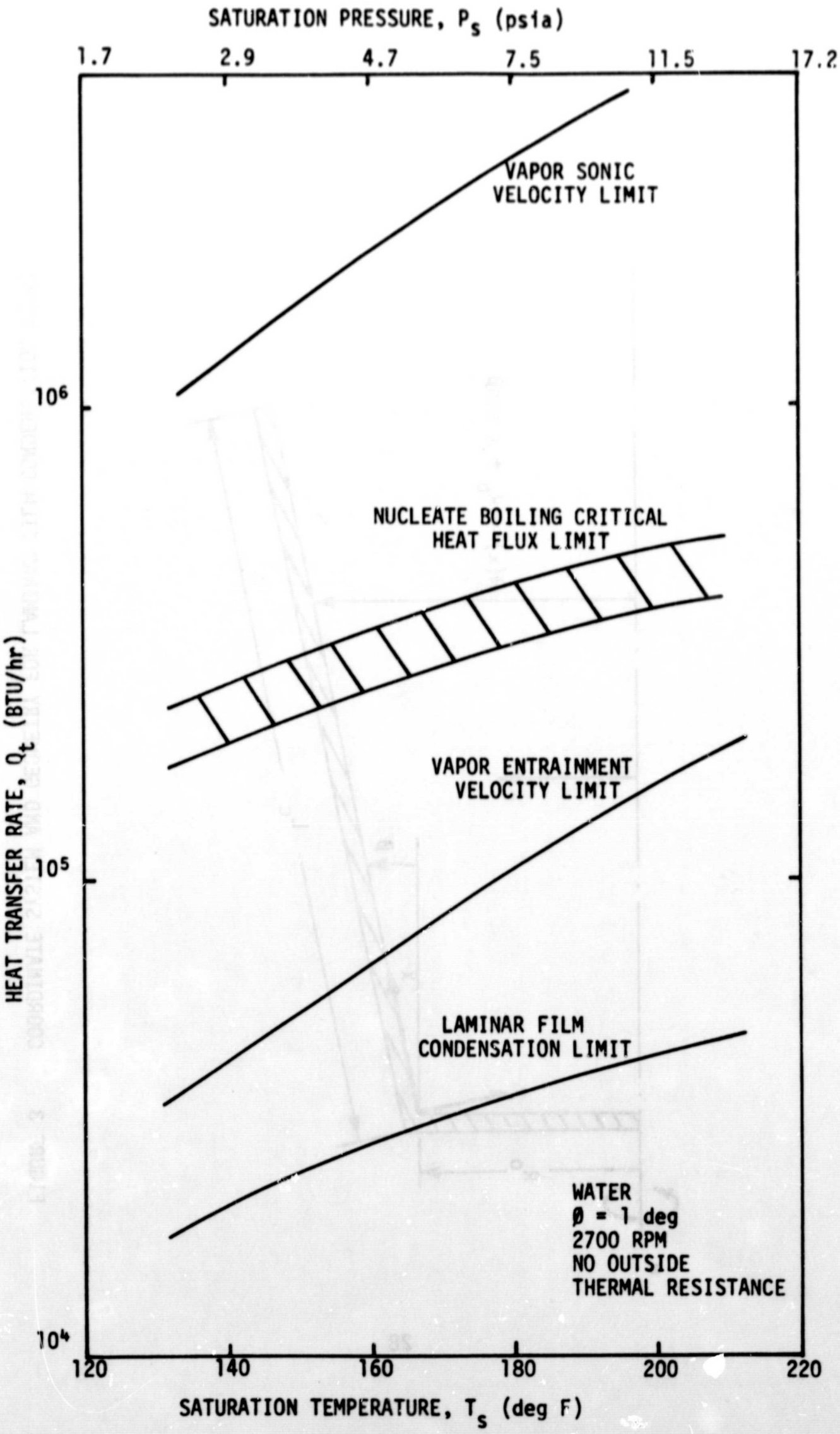

FIGURE 2 COMPARISON OF ROTATING HEAT PIPE LIMITATIONS

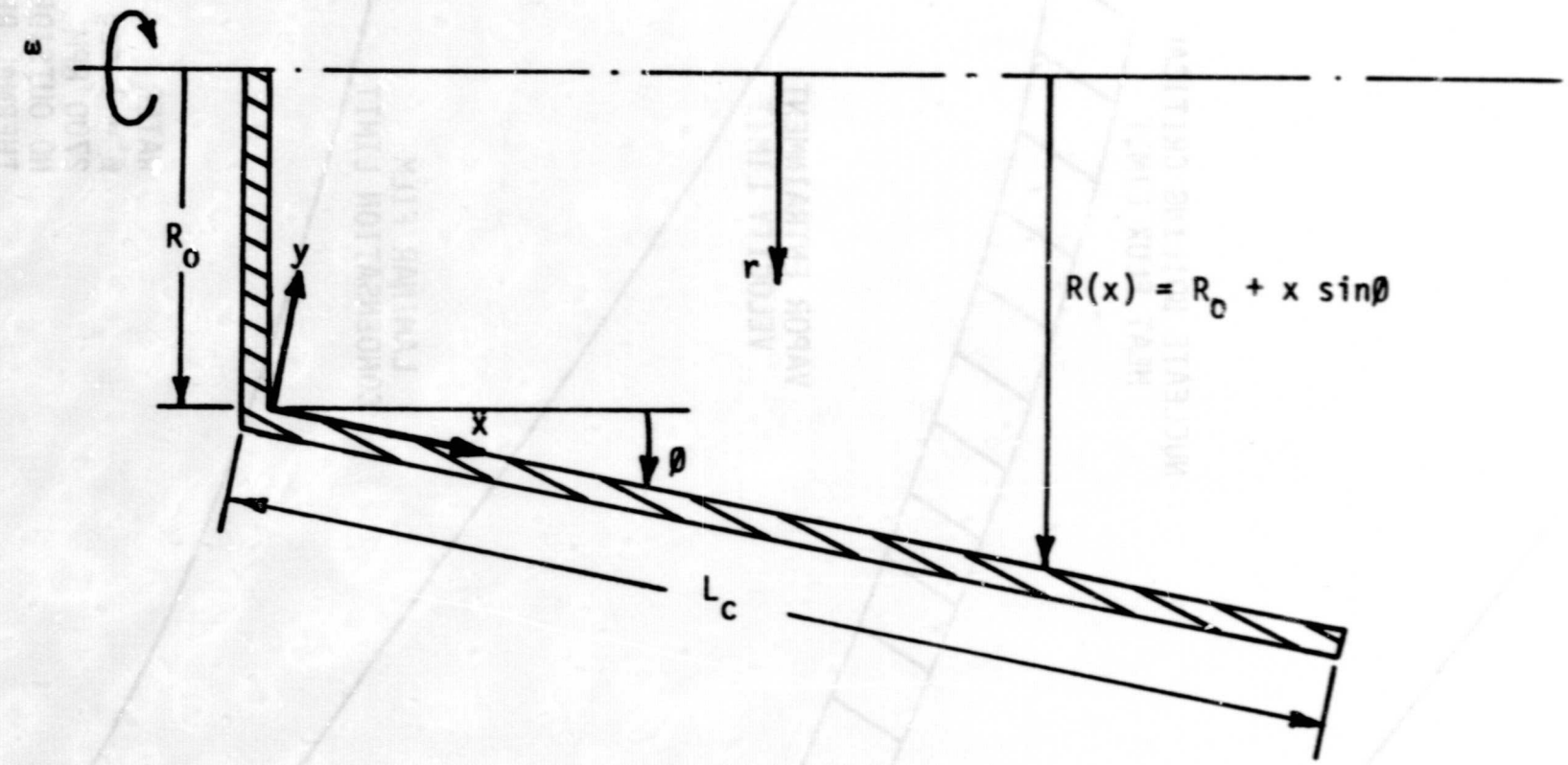

FIGURE 3 COORDINATE SYSTEM AND GEOMETRY FOR LAMINAR FILM CONDENSATION MODEL

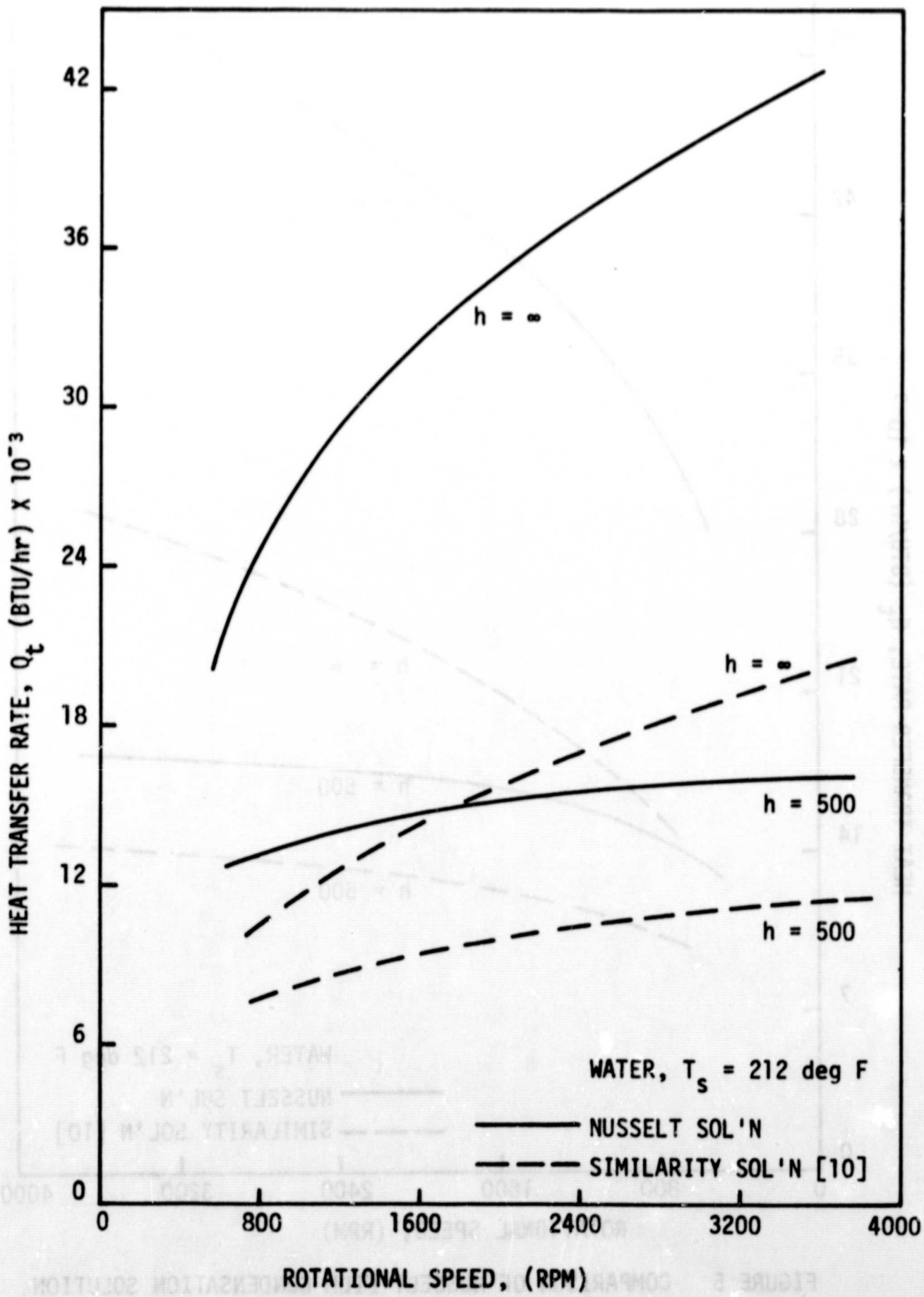

FIGURE 4 COMPARISON OF NUSSELT FILM CONDENSATION SOLUTION TO SPARROW AND HARTNETT [10] SIMILARITY SOLUTION FOR HALF-CONE ANGLE, ϕ = 1 DEGREE

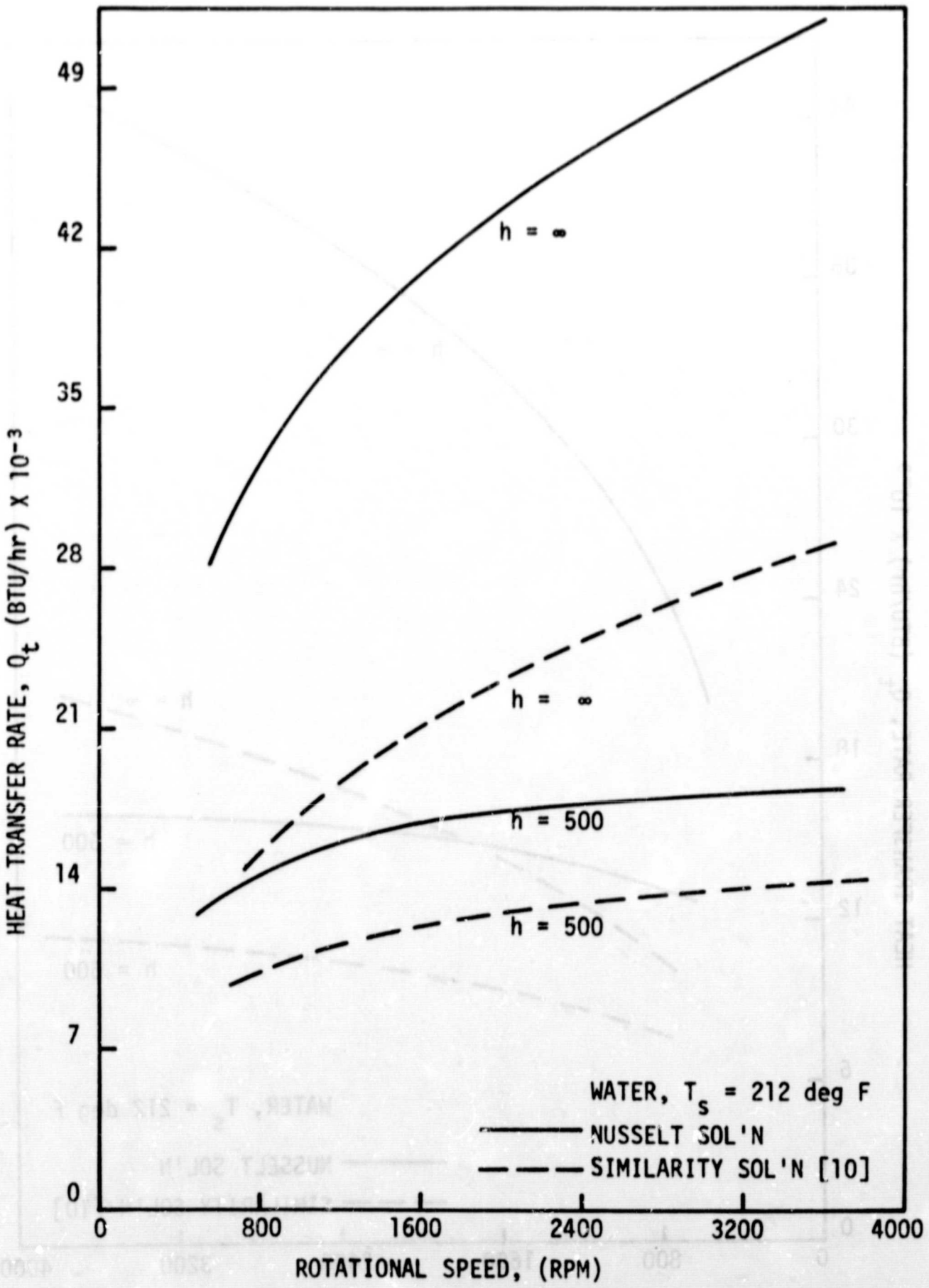

FIGURE 5 COMPARISON OF NUSSELT FILM CONDENSATION SOLUTION TO SPARROW AND HARTNETT [10] SIMILARITY SOLUTION FOR HALF-CONE ANGLE, $\emptyset$ = 2 DEGREES

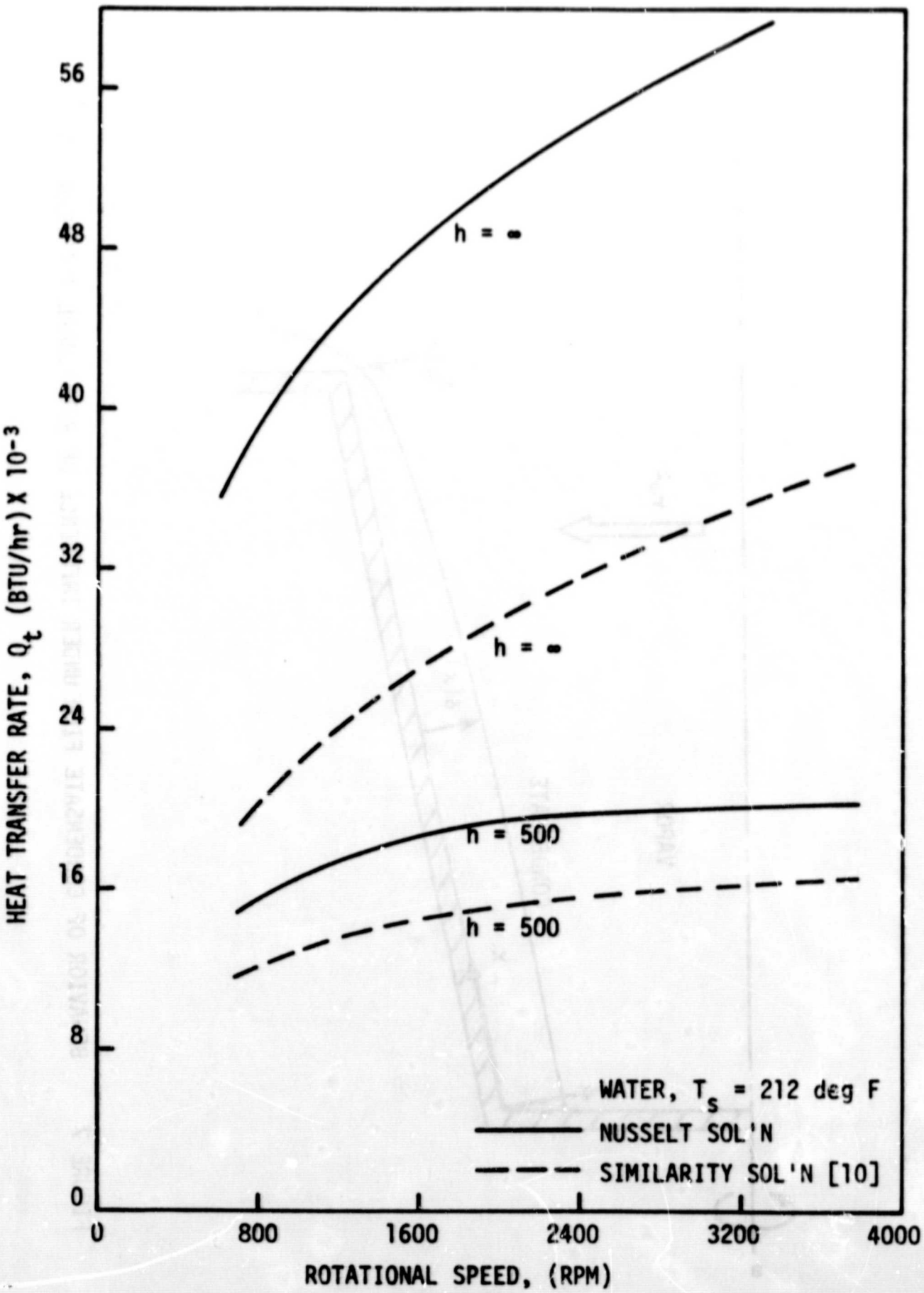

FIGURE 6 COMPARISON OF NUSSELT FILM CONDENSATION SOLUTION TO SPARROW AND HARTNETT [10] SIMILARITY SOLUTION FOR HALF-CONE ANGLE, $\emptyset$ = 3 DEGREES

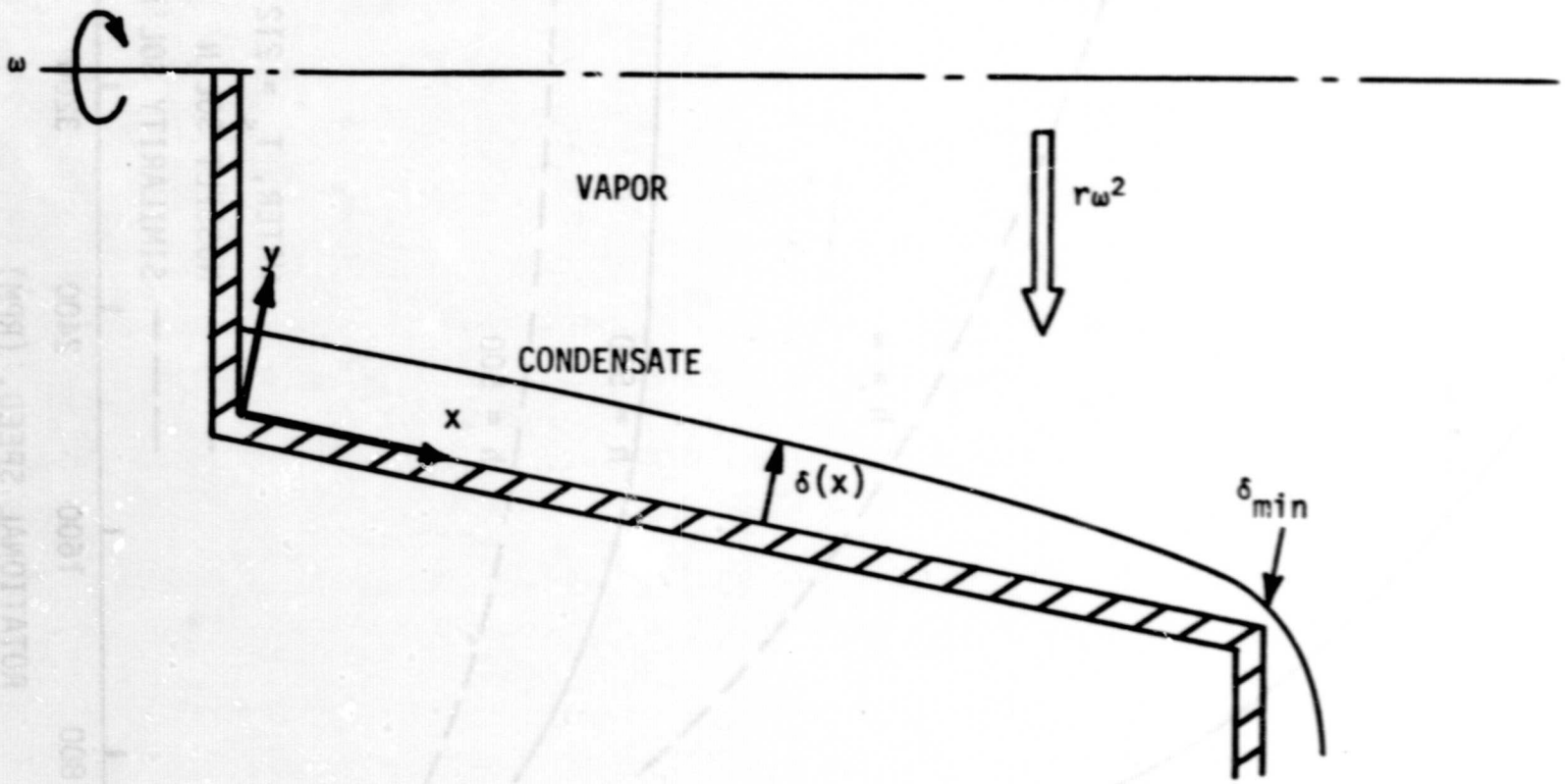

FIGURE 7 BEHAVIOR OF CONDENSATE FILM UNDER INFLUENCE OF ROTATIONAL ACCELERATION

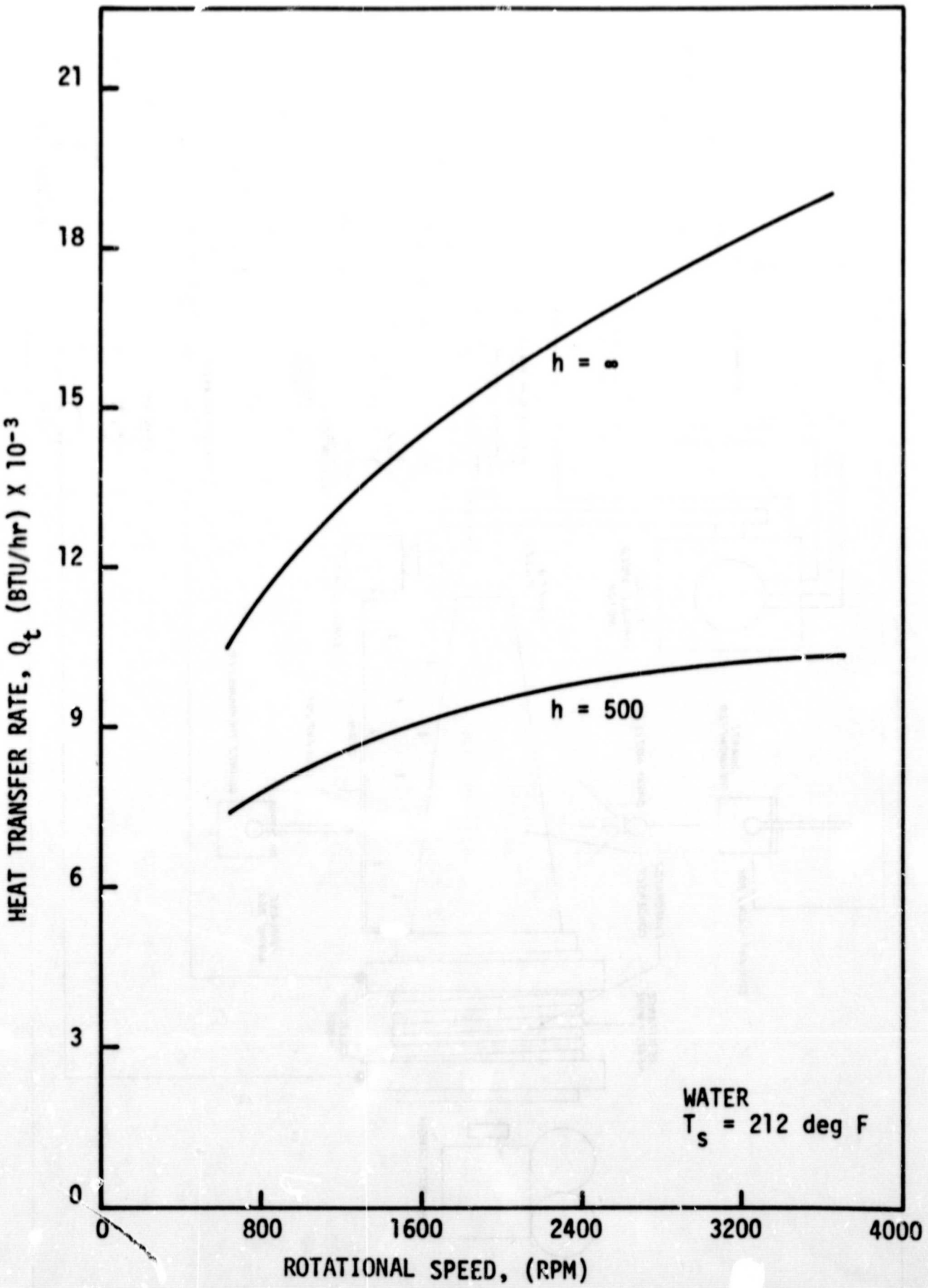

FIGURE 8 IMPROVED NUSSELT FILM CONDENSATION SOLUTION FOR ROTATING CYLINDER, ϕ = 0 DEGREES

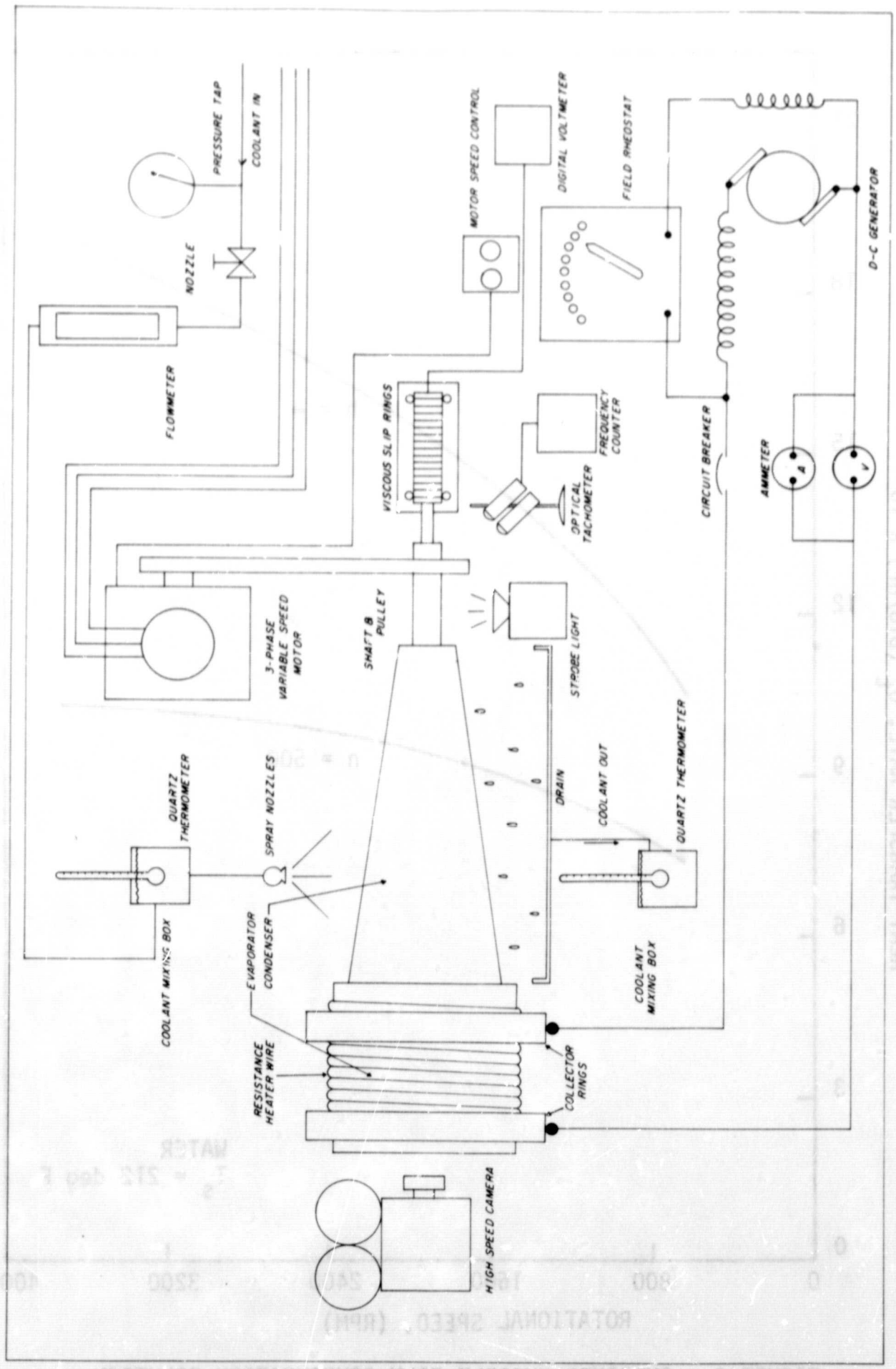

FIGURE 9 SCHEMATIC DIAGRAM OF APPARATUS

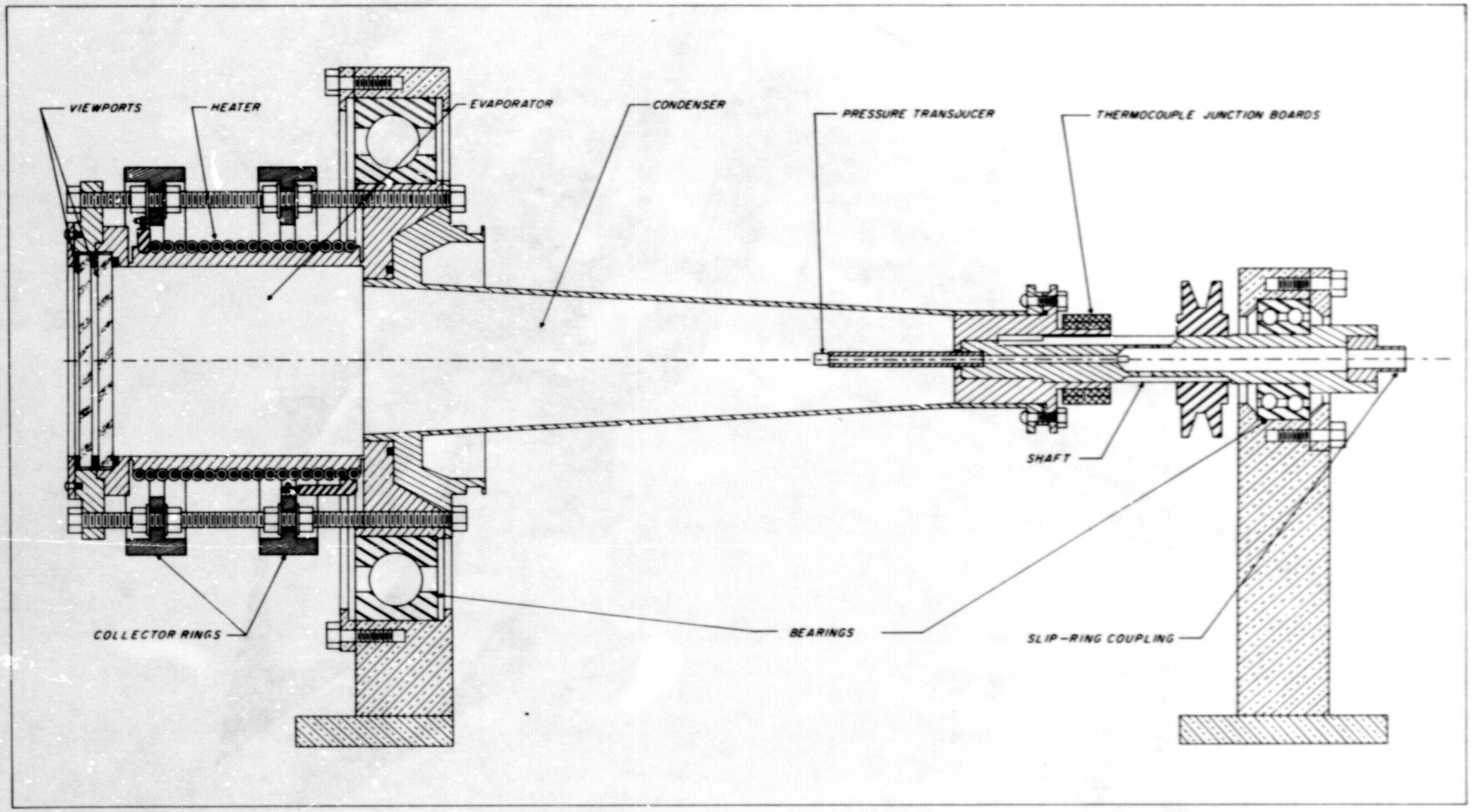

FIGURE 10 CROSS SECTION OF ROTATING HEAT PIPE

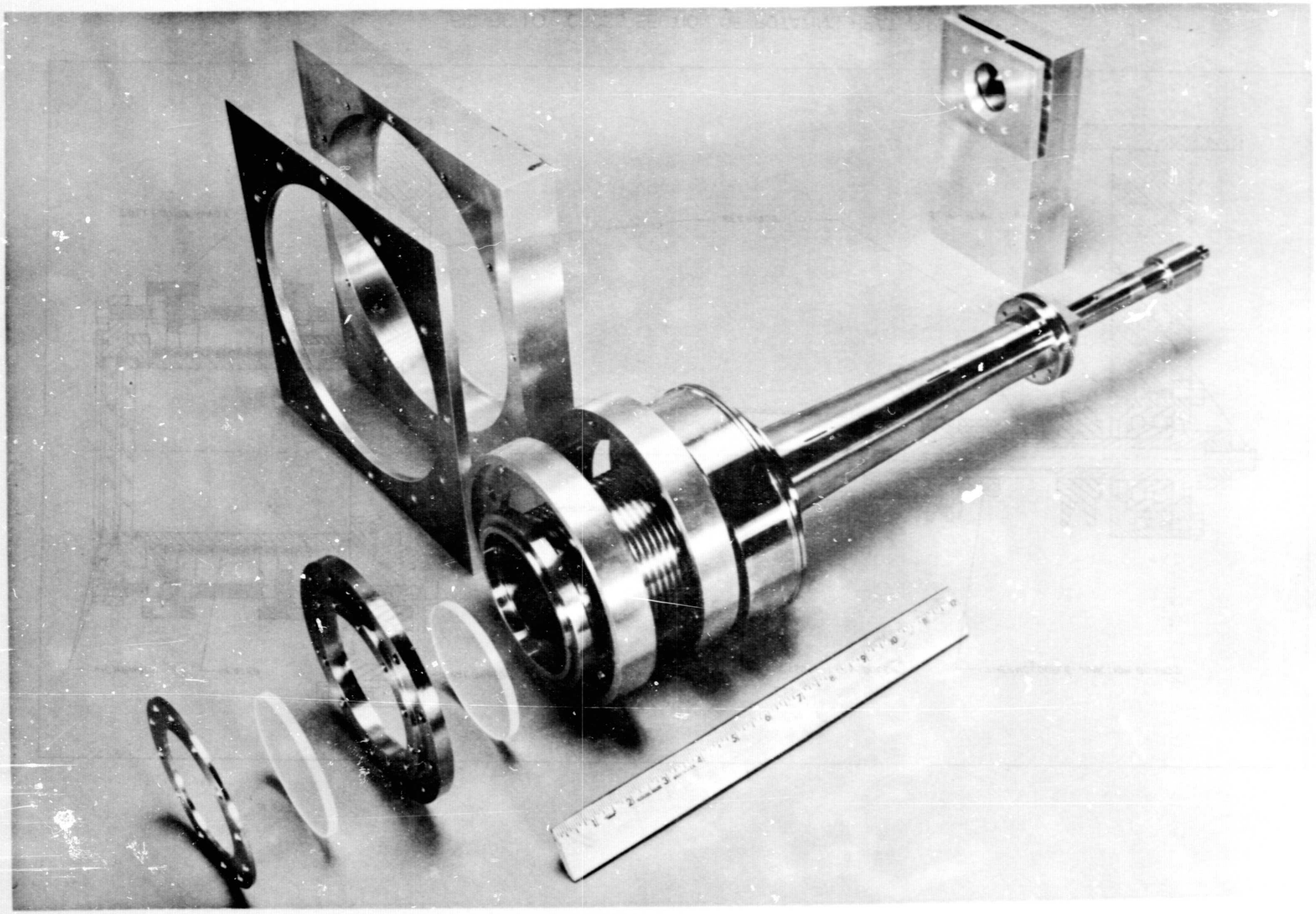

FIGURE 11 PHOTOGRAPH OF ROTATING HEAT PIPE COMPONENTS PRIOR TO ASSEMBLY

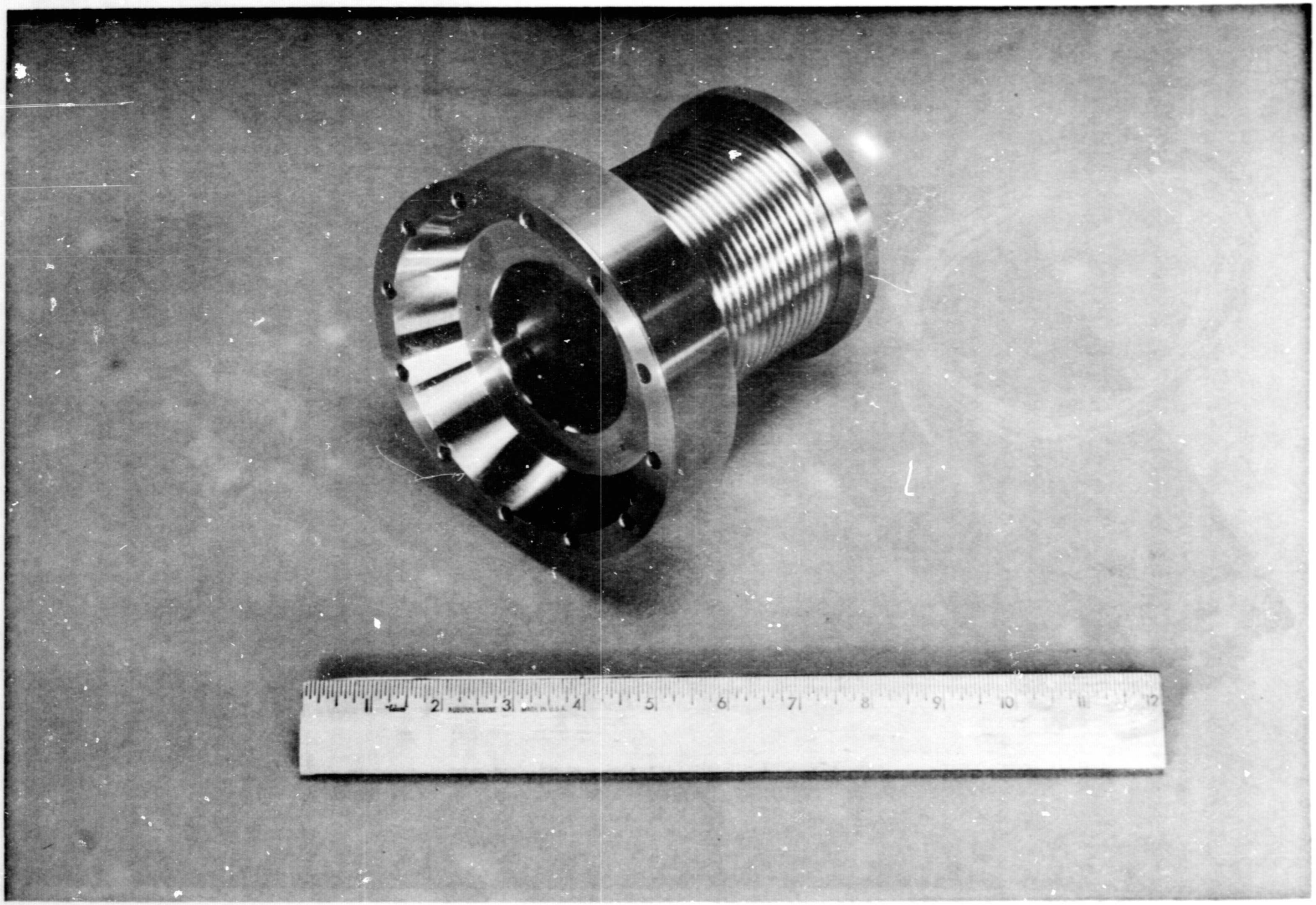

FIGURE 12 PHOTOGRAPH OF MACHINED EVAPORATOR SECTION

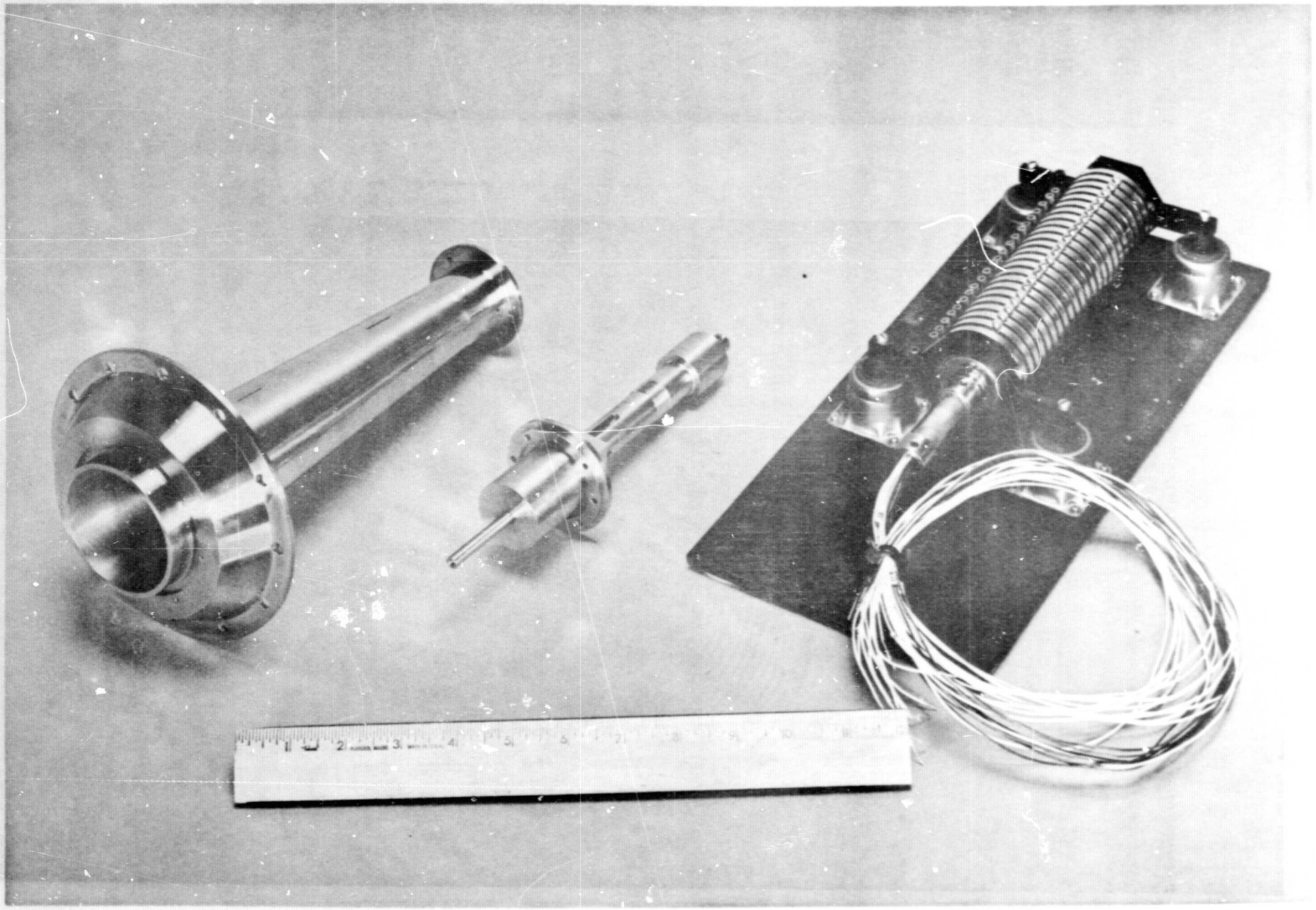

FIGURE 13 PHOTOGRAPH OF MACHINED CONDENSER SECTION WITH END PLUG AND SLIP-RING UNIT

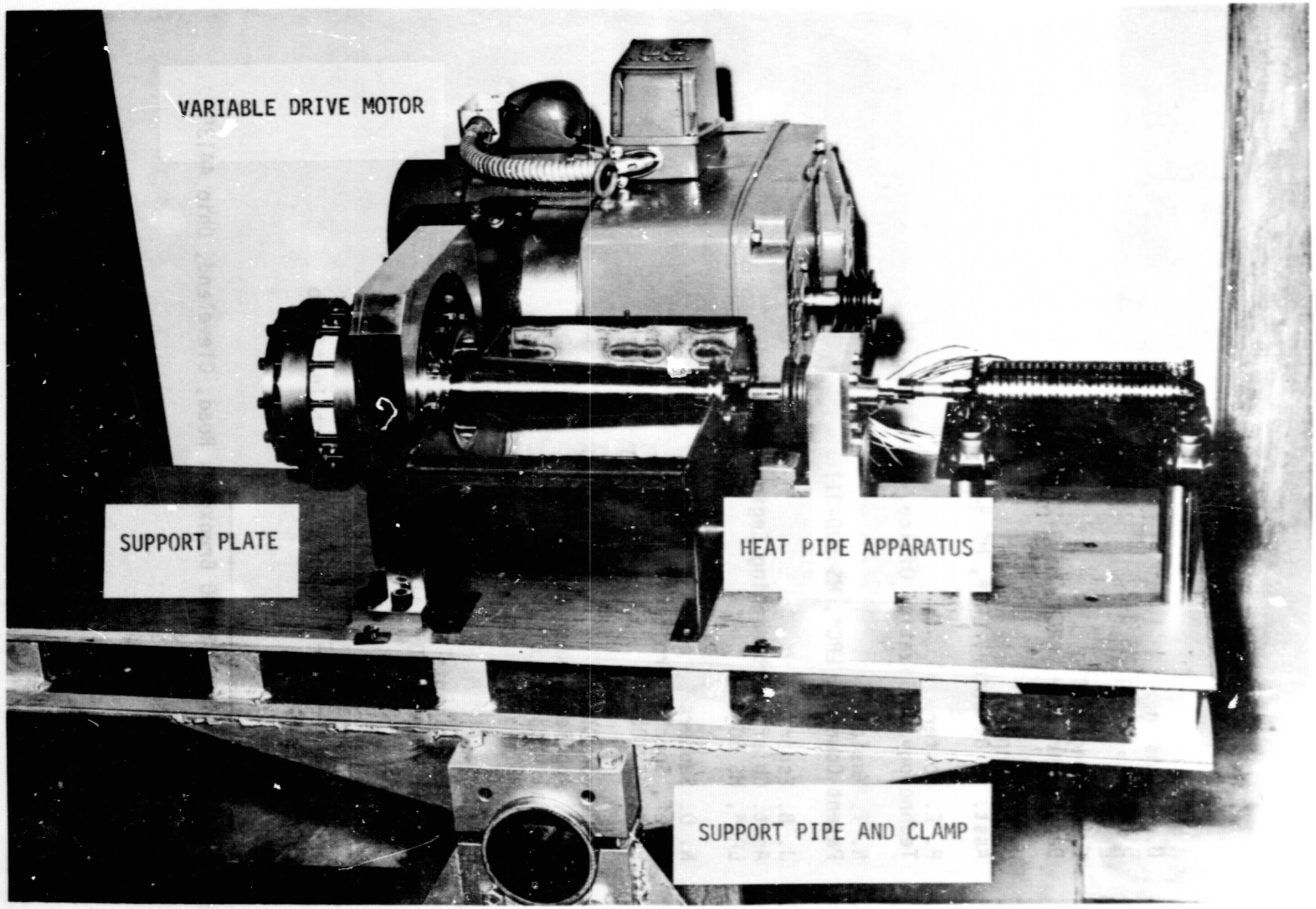

FIGURE 14 PHOTOGRAPH OF HEAT PIPE APPARATUS SHOWING TEST STAND